Advances in Biomechanics and Applications, *Vol. 1, No. 1 (2014) 067-076*
DOI: http://dx.doi.org/10.12989/aba.2013.1.1.067

The effect of mechanical properties of bone in the mandible, a numerical case study

António Ramos[*1], Hugo Marques[1] and Michel Mesnard[2]

[1]*TEMA, Department of Mechanical Engineering, University of Aveiro, Portugal*
[2]*University of Bordeaux, I2M, CNRS UMR 5295, Talence, France*

(Received March 9, 2013, Revised June 10, 2013, Accepted June 17, 2013)

Abstract. Bone properties are one of the key components when constructing models that can simulate the mechanical behavior of a mandible. Due to the complexity of the structure, the tooth, ligaments, different bones etc., some simplifications are often considered and bone properties are one of them. The objective of this study is to understand if a simplification of the problem is possible and assess its influence on mandible behavior. A cadaveric toothless mandible was used to build three computational models from CT scan information: a full cortical bone model; a cortical and cancellous bone model, and a model where the Young's modulus was obtained as function of the pixel value in a CT scan. Twelve muscle forces were applied on the mandible. Results showed that although all the models presented the same type of global behavior and proximity in some locations, the influence of cancellous bone can be seen in strain distribution. The different Young's modulus defined by the CT scan gray scale influenced the maximum and minimum strains. For modeling general behavior, a full cortical bone model can be effective. However, when cancellous bone is included, maximum values in thin regions increase the strain distribution. Results revealed that when properties are assigned to the gray scale some peaks could occur which did not represent the real situation.

Keywords: biomechanics; finite element method; modeling and simulation; dental mechanics; bone biomechanics

1. Introduction

Finite element models are used in the study of complex biomechanics structures, and they have the main advantage of reducing the need for animal experimentation (Wong *et al.* 2011). Biomechanical computational models are currently widely used and have proven to be a very useful tool to simulate bone behavior and other structures (Marinescu *et al.* 2005).

In the construction of biomechanical models, as in finite element models, it is necessary to assume the material properties and the geometry of the bone structure. Bone properties are one of the key components to consider when constructing models that can simulate the mechanical characteristics of the temporomandibular joint (TMJ) (Austman *et al.* 2008, Chen *et al.* 2010) or its behavior in different stages of life (Bujtar *et al.* 2010).

*Corresponding author, Professor, E-mail: a.ramos@ua.pt

 ISSN: 2287-2094 (Print), 2287-2272 (Online)

Due to the complexity of the mandible geometry, several models assume the bone properties as isotropic and homogenous (Yosibash *et al.* 2007, Huang *et al.* 2010), while others consider orthotropic properties. Other methods used in some specific cases consider that bone material is related to the radiographic density obtained from CT scanning (Zannoni *et al.* 1998).

This is a very common process (Liu *et al.* 2004, Tie *et al.* 2006, Helgason *et al.* 2008) and besides obtaining bone material properties, it is also able to differentiate internal tissues or different bone types (Sun and Lal 2002, Kalender 2006). By relating pixel values and bone mineral density (BMD) it is possible to estimate density (Zhang *et al.* 2002, Sato *et al.* 2005, Bujtár *et al.* 2010) from the results of the CT scan. This is a very practical tool since bone mechanical properties vary according to anatomical site, from person to person and species to species (Rho 1995, Helgason 2008).

Bone properties are extremely important when developing new medical devices, when studying, for example, the fixation phenomenon in TMJ implants (Chowdhury *et al.* 2011), or introducing a fixed plate into a condyle fracture (Parascandolo *et al.* 2010).

This work focuses on analysis of the influence of bone properties on mandible behavior. A numerical model of a cadaveric mandible was developed to determine whether the problem could be simplified. Different models with different material properties were simulated and their behavior compared.

2. Materials and methods

A cadaveric dry toothless mandible from Anatomy laboratory in Bordeaux, represented in figure 1, was used to build 3D computational models. The teeth were removed after death, and the mandible was cleaned. Therefore the models did not include the teeth and periodontal ligaments. The models were constructed based on the conversion of CT scans using Scan IP ® (Simpleware) software. The CT scanner was a Toshiba® Asteion CT data acquisition system and CT scans were made with a resolution of 0.315x0.315mm and 0.512mm of slice interval which was considered to be enough to accurately represent the mandible (Gröning *et al.* 2009).

Three models were developed with the same CT Scan;

Model (I) - a full cortical bone model, including cancellous bone with same bone properties (E=15750MPa, ν=0.325). This model considers all bone structure as a cortical bone.

Model (II) - a model with cortical and cancellous bone modeled separately, using cortical bone properties (E=15750MPa, ν=0.325) and cancellous bone properties (E=300MPa, ν=0.30) obtained from a previous study (Reina-Romo *et al.* 2010). All bone areas were divided into separate cortical and cancellous bone regions by thresholding of the grey levels. The cortical bone was considered with a threshold of 80% of the peak height in the profile-scan according other studies (Iwashita 2000).

Model (III) - a model where the Young's modulus was obtained as function of the pixel value.

The first two models consider the cortical and cancellous bone as homogenous and isotropic. The bone properties for the gray scale model were obtained using linear relationships. Bone mineral density (BMD) Eq. (1) was estimated from a linear relationship between pixel values and BMD (Zhang *et al.* 2002)

$$BMD\left(\frac{g}{cm^3}\right) = 0.012 \times \text{Pixel value} + 1.005 \quad (1)$$

Fig. 1 Cleaned cadaveric mandible

A linear relationship between BMD and the Young's modulus, eq. (II) was used to obtain the Young modulus (Zhang *et al.* 2002) considering the maximum bone properties of cortical bone defined in model (I and II):

$$E_{(MPa)} = 9.482 \times 10^{8} \times \rho_{\left(\frac{kg}{mm^3}\right)} \tag{2}$$

2.1 Finite element analysis

The mesh was constructed using four node tetrahedral elements in the ScanFE from Simpleware 5.0 version and MSC MarcTM 2012 software was used to solve the simulations. The mesh properties for each model are presented in Table 1.

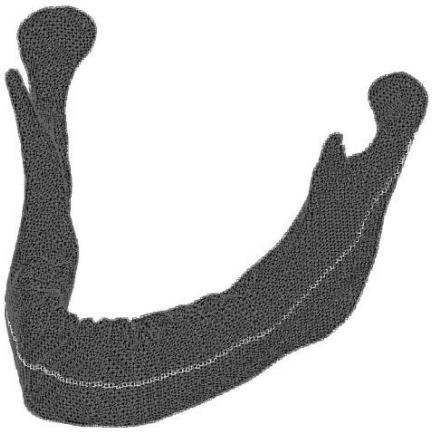

Fig. 2 Mesh model with control line

Table 1 Number of elements and nodes for each model

	Model (I)	Model (II)	Model (III)
Elements	175068	186246	175068
Nodes	41539	44840	41539

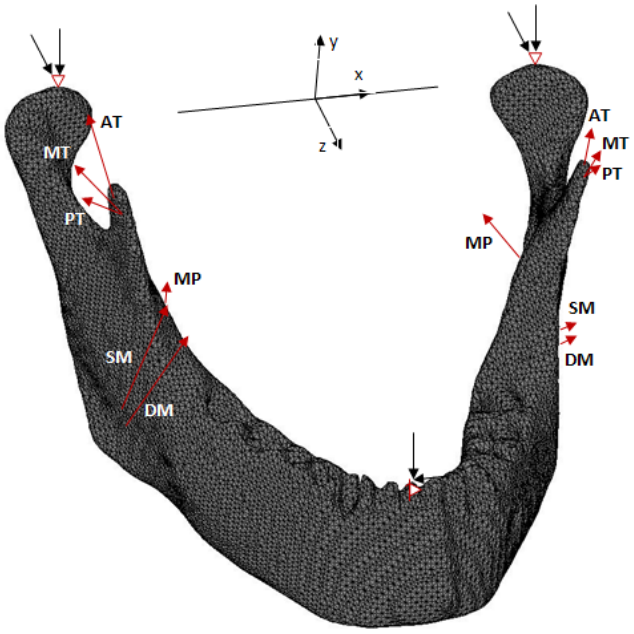

Fig. 3 Boundary conditions

2.2 Boundary conditions

The mandible was constrained in three locations as in previous studies (Ramos *et al.* 2011). The condyles were fixed on the *y* and *z* axes (Fig. 3). The other support was the position of incisive tooth (same position because the model is toothless) with constraints in the *y* and *x* directions. Twelve muscle forces (six on each side) were applied to the mandible (Mesnard 2005, Mesnard *et al.* 2011). The values applied for each force can be seen in Table 2.

3. Results

Maximum and minimum principal strain and displacement values were obtained for each model. Model (I) presented the lowest maximum (Fig. 4) and minimum principal strain values (Fig. 5) at most locations. The difference was more pronounced between the left and right ramus, showing a good approximation with model (III) near the condyles. The average value for the maximum strain between rami was 632μstrain for model (I) and 863 μstrain for model (III). This means the average difference was around 27.8% in this area.

Table 2 Muscle forces

	Load (N)		
	X	Y	Z
Superficial Masseter (SM)	18,2	303,3	12,1
Deep Masseter (DM)	7,8	128,3	15,6
Anterior Temporalis (AT)	-18,4	104,8	-43,8
Medial Temporalis (MT)	-6,5	36,3	-53,1
Posterior Temporalis (PT)	-3,4	6,8	-37
Medial Pterygoid (MP)	187,4	325,1	-76,5

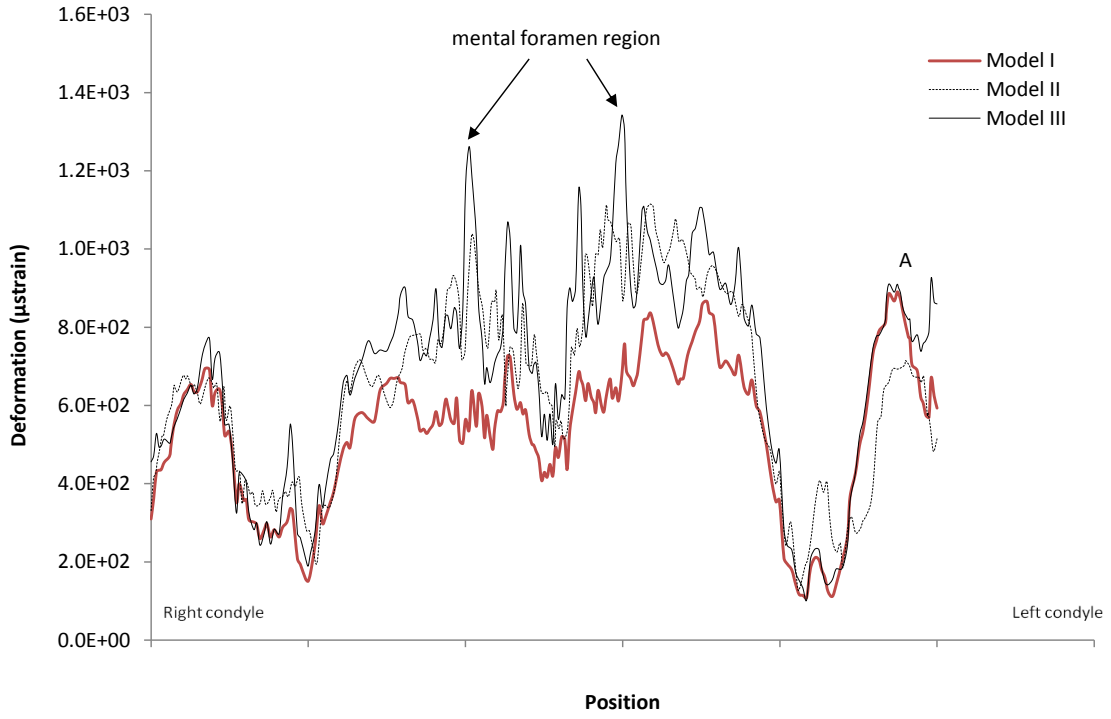

Fig. 4 Maximum strains distribution in the control line

The highest peak in model (I) for the maximum principal strain was at 890μstrain (point A), near the left condyle. Models (II) and (III) showed similar strain values (Fig. 4) in most locations, except near the left condyle and in some peaks. The maximum values were near the left mental foramen and were 1110μstrain for model (II) and 1340μstrain for model (III).

For the minimal principal strain, the difference between models was more pronounced, because the mandible was mainly in compression. The average value for minimal strain between rami was -1290μstrain for model (I), -1580μstrain for model (II) and -1910μstrain for model (III). The

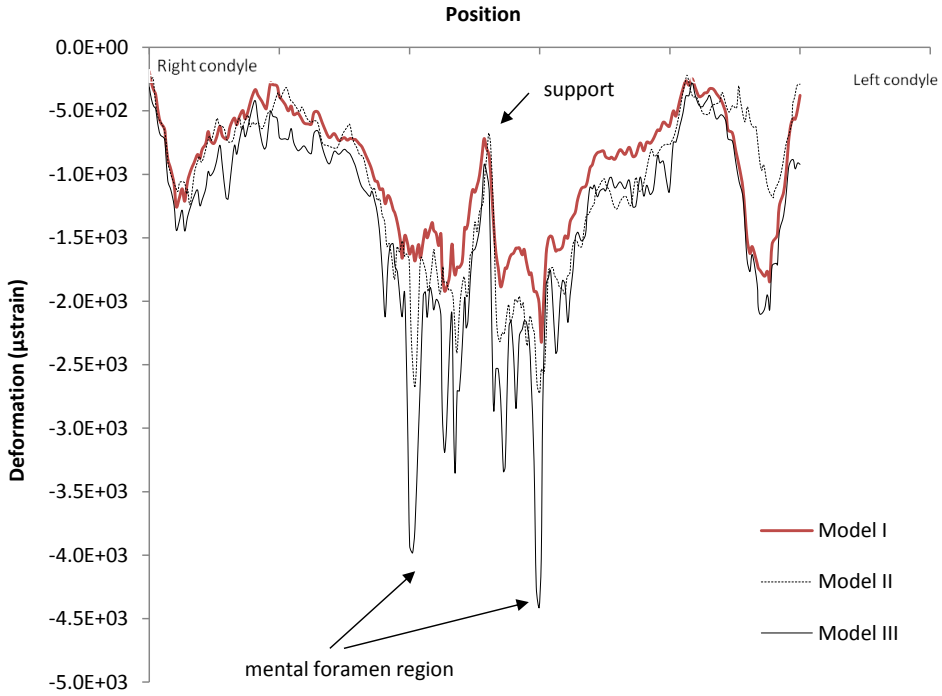

Fig. 5 Minimum strains distribution in the control line

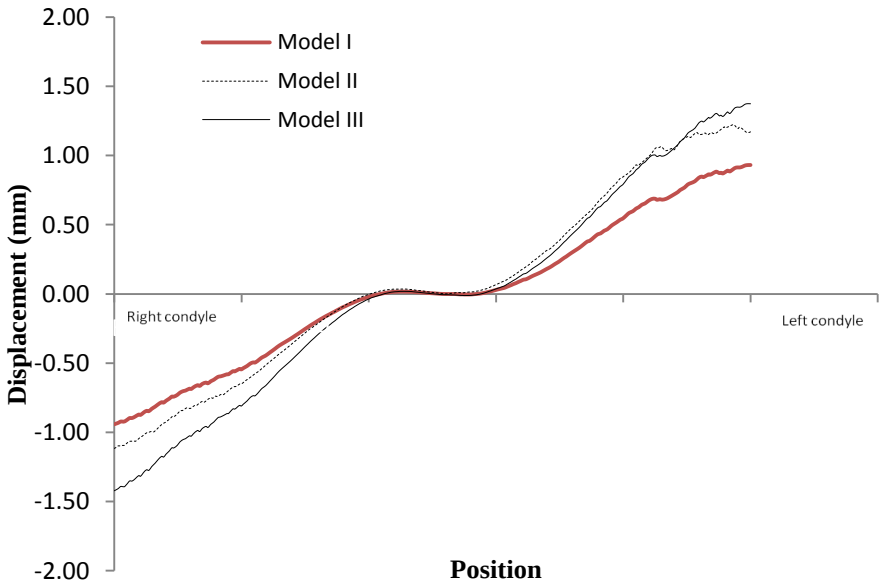

Fig. 6 Displacement *x* direction in control line

average difference was around 32.4% for model (I) and 1.7% for model (II). The highest peak value for the minimal principal strain was -2320μstrain for model (I), located near the left mental foramen. For model (II) it was -2720μstrain and for model (III) -4410μstrain.

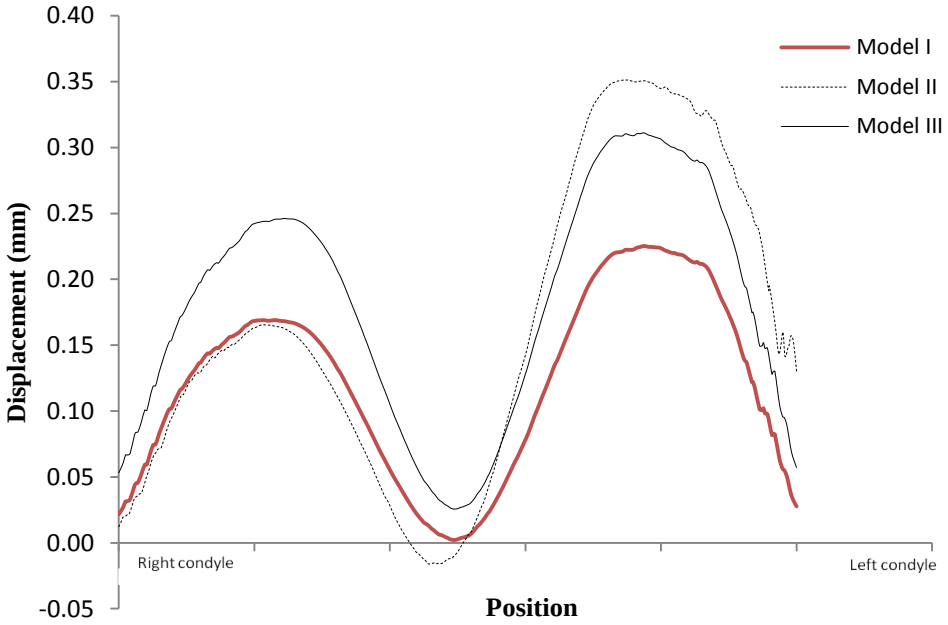

Fig. 7 Displacement *y* direction in control line

Table 3 Maximum displacement in the condyles

		Displacement (mm)		
	Model	X	Y	Z
Right condyle	I	-0.89	0.05	0.12
	II	-1.06	0.04	0.12
	III	-1.34	0.09	0.19
Left condyle	I	0.90	0.07	0.15
	II	1.19	0.17	0.26
	III	1.33	0.11	0.22

Displacements for the *x*- and *y*-directions are shown in Figs. 6 and 7. The results for *x*-direction were similar in the left condyle for model (II) and model (III). Displacements in model (I) are lower in this direction compared with the other models (33% difference). The results revealed some influence of cancellous bone geometry in the left condyle, and in some regions values in model (I) were higher than in the other models.

In the *y*-direction, the influence of bone properties is not so well defined (Fig. 7). Model (I) presents lower displacements in the left condyle, but in the right condyle model (II) presents the lowest values. Model (II), on the other hand, presents the highest values in the left condyle. Displacements in the *y*-direction are lower than in the *x*-direction, with differences of 0.351 for model (II) and 0.225 for model (I) (55%).

In the *z*-direction, displacement is similar to that in the *y*-direction, with model (II) presenting

greater displacement in the left condyle (79% of difference). In the right condyle the differences are not so significant and displacements in models (I) and (II) are similar. The maximum displacement near the condyles for different directions is presented in Table 3.

4. Discussion

The results presented here reveal in all cases non-symmetric mandible behavior in terms of strain and displacements, although the models present the same global behavior with different maximum values (Figs. 4 and 5). This agrees with other previous studies (Panagiotopoulou *et al.* 2010) which concluded that full cortical bone models give a good concordance, but differ in some locations. The non-symmetric mandible behaviour was explained by the mandible geometry, not by the boundary conditions or different model constructions.

It is clear that the peak locations were the same in all models, but model (III) with assigned bone properties presented a higher strain value, especially in minimum principal strains. The presence of pixels from CT scan with a small gray scale value in some regions originates elements (volumes) with a low Young's modulus. The different Young's modulus at these locations influences the maximum and minimum principal strains, increasing the values. The peak values are not correct as they exceed the maximum values before micro-cracks appear in bone around 4000μ strain (Roberts *et al.* 2004)

For example, in the frontal region of the mandible, a high level of strain was observed; we analyzed what could influence this in the model and observed that variation in bone properties were around 3 times less in these elements. Using homogeneous bone properties as a cortical bone reduces the peaks of strain in the mandible, and maintains the same global behavior.

Concerning displacements, Model (II), which was influenced by the stiffness, showed more displacement on the left condyle in the three directions; this suggests the importance of defining the cancellous bone geometry in models, as it could change displacement in your model by 55% (*y*-direction) and 79% in *z* direction. The definition of the two materials needs to be considered carefully, because this could change model behavior. In this case a uniform bone property model presents more stable mandible behavior.

5. Conclusions

Considering the results obtained, the maximum and minimum strains are directly influenced by the bone properties. The strain results for the three models were closer near the condyles; however, the model with assigned bone properties presented a higher strain value in most locations. This difference can be explained by the presence of pixels with a low gray scale value. For modeling the general behavior of mandible, defined full cortical bone model with homogeneous young modulus properties can be effective to represent the uniform model behavior.

Acknowledgments

The authors acknowledge the Portuguese Science and Technology Foundation for funding project PTDC/EME-PME/112977/2009 which support the research.

References

Austman, R.L., Milner, J.S., Holdsworth, D.W. and Dunning, C.E. (2008), "The effect of the density–modulus relationship selected to apply material properties in a finite element model of long bone", *J. Biomech.*, **41**(3), 171-3176.

Bujtar, P., Sandor, G.K., Bojtos, A., Szucs, A. and Barabas, J. (2010), "Finite element analysis of the human mandible at 3 different stages of life", *Oral Surg. Oral Med. O.*, **110**(3), 301-309.

Chen, G., Schmutz, B., Epari, D., Rathnayaka, K., Ibrahim, S., Schuetz, M.A. and Pearcy, M.J. (2010), "A new approach for assigning bone material properties from CT images into finite element models", *J. Biomech.*, **43**(5), 1011-1015.

Chowdhury, A.R., Kashi, A. and Saha, S. (2011), "A comparison of stress distributions for different surgical procedures, screw dimensions and orientations for a Temporomandibular joint implant", *J. Biomech.*, **44**(14), 2584-2587.

Gröning, F., Liu, J., Fagan, M.J. and O'Higgins, P. (2009), "Validating a voxel-based finite element model of a human mandible using digital speckle pattern interferometry", *J. Biomech.*, **42**(9), 1224-1229.

Helgason, B., Perilli, E, Schileo, E., Taddei, F., Brynjolfsson, S. and Viceconti, M. (2008), "Mathematical relationships between bone density and mechanical properties: a literature review", *Clin. Biomech.*, **23**(2), 135-146.

Helgason, B., Taddei, F., Palsson, H., Schileo, E., Cristofolini, L., Viceconti, M. and Brynjolfsson, S. (2008), "A modified method for assigning material properties to FE models of bones", *Med. Eng. Phys.*, **30**(4), 444-453.

Huang, H.L., Tsai, M.T., Lin, D.J., Chien, C.S. and Hsu, J.T. (2010), "A new method to evaluate the elastic modulus of cortical bone by using a combined computed tomography and finite element approach", *Comput. Biol. Med.*, **40**(4), 464-468.

Kalender, W. A. (2006), "X-ray computed tomography", *Phys. Med. Biol.*, **51**, 29-43.

Iwashita, Y. (2000), "Basic study of the measurement of bone mineral content of cortical and cancellous bone of the mandible by computed tomography", *Dentomaxillofac. Rad*., **29**, 209-215.

Liu, J.G., Li, D.S., Ma, W.H., Zhou, Z.P. and Xu, X.X. (2004), "Computer assisted reconstruction of 3D canal model of femur and design for custom-made stem", *Chin. Med. J.***117**(8), 1265-1267.

Marinescu, R., Daegling, D.J. and Rapoff, A.J. (2005), "Finite-element modeling of the anthropoid mandible: the effects of altered boundary conditions", *Anat. Rec. Part A*, **283**(2), 300-309.

Mesnard, M. (2005), *Elaboration et validation d'un protocol de caractérisation de l'Articulation Temporo-Mandibulaire*, University Bordeux, IST Press.

Mesnard, M., Ramos, A., Ballu, A., Morlier, J. Cid, M. And Simoes, J.A. (2011), "Biomechanical analysis comparing natural and alloplastic temporomandibular joint replacement using a finite element model", *J. Oral Maxil. Surg.*, **69**(4), 1008-1017.

Panagiotopoulou, O., Curtis, N., O'Higgins, P. and Cobb, S.N. (2010), "Modelling subcortical bone in finite element analyses: a validation and sensitivity study in the macaque mandible", *J. Biomech.*, **43**(8), 1603-1611.

Parascandolo, S., Spinzia, A., Piombino, P. and Califano, L. (2010), "Two load sharing plates fixation in mandibular condylar fractures: biomechanical basis", *J. Cranio Maxill. Surg.*, **38**(5), 385-390.

Ramos, A., Completo, A., Relvas, C., Mesnard. M. and Simoes, J.A. (2011), "Straight, semi-anatomic and anatomic TMJ implants: the influence of condylar geometry and bone fixation screws", *J. Cranio Maxill. Surg.*, **39**(5), 343-350.

Reina-Romo, E., Sampietro-Fuentes, A., Gomez-Benito, M.J., Dominguez, J., Doblare, M. And Garcia-Aznar, J.M. (2010), "Biomechanical response of a mandible in a patient affected with hemifacial microsomia before and after distraction osteogenesis", *Med. Eng. Phys.*, **32**, 860-866.

Rho, J.Y., Hobatho, M.C., and Ashman, R.B. (1995), "Relations of mechanical properties to density and CT numbers in human bone", *Med. Eng. Phy*., **17**(5), 347-355.

Roberts, W.E., Huja, S. and Roberts, J.A. (2004), "Bone modeling: biomechanics, molecular mechanisms,

and clinical perspectives", *Semin. Orthod.*, **10**(2), 123-161.
Sato, H., Kawamura, A., Yamaguchi, M. and Kasai, K. (2005), "Relationship between masticatory function and internal structure of the mandible based on computed tomography findings", *Am. J. Orthod. Dentofac.*, **128**(6), 766-773.
Sun, W. and Lal, P. (2002), "Recent development on computer aided tissue engineering - a review", *Comp. Methods Programs Biomed*., **67**(2), 85-103.
Tie, Y., Ma, R., Ye, M., Wang, D. and Wang. C. (2006), "Rapid prototyping fabrication and finite element evaluation of 3D medical pelvic model", *Int. J. Adv. Manuf. Tech.*, **28**(3-4), 302-306.
Wong, R.C., Tideman, H., Merkx, M.A., Jansen, J., Goh, S.M. and Liao, K. (2011), "Review of biomechanical models used in studying the biomechanics of reconstructed mandibles", *Int. J. Oral Maxil. Surg.*, **40**, 393-400.
Yosibash, Z., Trabelsi, N. and Milgrom, C. (2007), "Reliable simulations of the human proximal femur by high-order finite element analysis validated by experimental observations", *J. Biomech.*, **40**(16), 3688-3699.
Zannoni, C., Mantovani, R. and Viceconti, M. (1998), "Material properties assignment to finite element models of bone structures: a new method", *Med. Eng. Phy*., **20**(10), 735-740.
Zhang, F., Peck, C.C. and Hannam, A.G. (2002), "Mass properties of the human mandible", *J. Biomech.*, **35**(7), 975-978.

YY